Magnetic Excitations and their energy change available to Superconducting Condensation in Optimally Doped YBa$_2$Cu$_3$O$_{6.95}$

Hyungje Woo,[1, 2] Pengcheng Dai,[1, 2] S. M. Hayden,[3] H. A. Mook,[2]
T. Dahm,[4] D. J. Scalapino,[5] T. G. Perring,[6] and F. Doğan[7]

[1] *Department of Physics and Astronomy, The University of Tennessee, Knoxville, Tennessee 37996-1200, USA*
[2] *Center for Neutron Scattering, Oak Ridge National Laboratory, Oak Ridge, Tennessee 37831, USA*
[3] *H. H. Wills Physics Laboratory, University of Bristol, Bristol BS8 1TL, UK*
[4] *Institut für Theoretische Physik, Universität Tübingen,*
Auf der Morgenstelle 14, D-72076 Tübingen, Germany
[5] *Department of Physics, University of California, Santa Barbara, California 93106, USA*
[6] *ISIS Facility, Rutherford Appleton Laboratory, Chilton, Didcot, Oxon, OX11 0QX, UK*
[7] *Department of Ceramic Engineering, University of Missouri-Rolla, Rolla, Missouri 65409-0330, USA*

Understanding the magnetic excitations in high-transition temperature (high-T_c) copper oxides is important because they may mediate the electron pairing for superconductivity [1, 2]. By determining the wavevector (Q) and energy ($\hbar\omega$) dependence of the magnetic excitations, one can calculate the change in the exchange energy available to the superconducting condensation energy [3, 4, 5]. For the high-T_c superconductor YBa$_2$Cu$_3$O$_{6+x}$, the most prominent feature in the magnetic excitations is the resonance [6, 7, 8, 9, 10, 11, 12]. Although the resonance has been suggested to contribute a major part of the superconducting condensation [4, 13], the accuracy of such an estimation has been in doubt because the resonance is only a small portion of the total magnetic scattering [12, 13, 14]. Here we report an extensive mapping of magnetic excitations for YBa$_2$Cu$_3$O$_{6.95}$ ($T_c \approx 93$ K). Using the absolute intensity measurements of the full spectra, we estimate the change in the magnetic exchange energy between the normal and superconducting states and find it to be about 15 times larger than the superconducting condensation energy [15, 16]. Our results thus indicate that the change in the magnetic exchange energy is large enough to provide the driving force for high-T_c superconductivity in YBa$_2$Cu$_3$O$_{6.95}$.

If magnetic excitations are mediating electron pairing in the high-T_c copper oxides, one expects that the change in magnetic exchange energy provides enough energy for superconducting condensation. The condensation energy is known experimentally from specific heat measurements for YBa$_2$Cu$_3$O$_{6.95}$ (YBCO) to be ∼3 K/formula unit (f.u.) [15, 16]. Within the t-J model the change in magnetic exchange energy can be calculated from the nearest neighbor spin correlations [3, 4, 5]:

$$\Delta E_{ex} = 2J \left(\left\langle \vec{S}_i \cdot \vec{S}_j \right\rangle_S - \left\langle \vec{S}_i \cdot \vec{S}_j \right\rangle_N \right) \quad (1)$$

where J is the exchange interaction, $\vec{S}_i$ and $\vec{S}_j$ are the electron spin operators at nearest neighbor Cu sites i and j in the CuO$_2$ plane, respectively. Instead of estimating the magnetic resonance's contribution to the superconducting condensation [4, 13], we seek here to calculate ΔE_{ex} from the entire observable magnetic excitation spectrum. In general, a complete determination of the magnetic excitation spectrum is difficult as spin fluctuations can spread over a large wavevector and energy range. YBCO has two CuO$_2$ planes per unit cell (bilayer) and therefore the magnetic excitations have odd (acoustic) or even (optical) symmetry with respect to the neighboring planes (Fig. 1). For optimally doped YBCO, the magnetic excitation spectrum is dominated by a resonance mode centered at 41 meV in the acoustic channel [6, 7], and a mapping of the acoustic and optical magnetic excitations should allow an estimation of ΔE_{ex}.

Figure 1 summarizes the key conclusions of our work. The optical and acoustic spin fluctuations can be separated by their differences in q_z-dependence (Fig. 1b). The total magnetic response $\chi''(Q, \omega)$ can then be written as $\chi''(q_x, q_y, q_z, \omega) = \chi_a''(q_x, q_y, \omega) \sin^2(q_z d/2) + \chi_o''(q_x, q_y, \omega) \cos^2(q_z d/2)$, where $d = 3.342$ Å is the spacing between the nearest neighbor CuO$_2$ planes along the c-axis. To probe the entire magnetic spectra in optical and acoustic channels of YBCO, we used the MAPS spectrometer at ISIS Facility [12, 17] and chose incident beam energies of $E_i = 30$, 40, 62.5, 75, 90, 110, 130, 138, 160, 210, 280, 360, and 450 meV with the incident beam along the c-axis. The position sensitive detectors on MAPS allow a complete determination on the **Q**-structure of incommensurate spin fluctuations for YBCO in one experimental setting [12]. This avoids the complication of de-convoluting the instrumental resolution necessary for structure determination of incommensurate peaks using triple-axis spectroscopy [18]. The temperatures probed were $T = 15$, 100, and 290 K. The intensity difference between 15 K and 100 K is almost entirely magnetic because of the small value of Q^2 probed by the experiment and small change in the Bose factor for $\hbar\omega > 30$ meV [9, 10, 19].

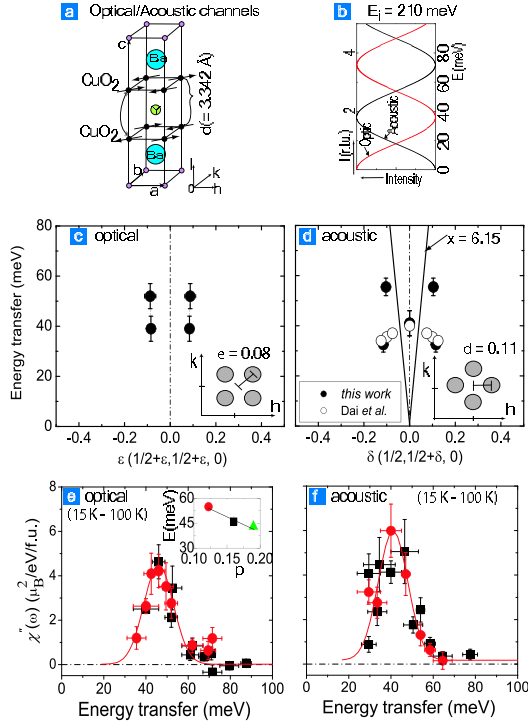Figures 2(a)-(c) summarize the temperature depen-

FIG. 1: Summary of **Q**- and ω-dependence of dynamic susceptibility for YBCO. Our experiments were carried out on the $\sim$117-g YBCO single crystal ($T_c = 92.5$ K) used in previous work [10]. We specify the momentum transfer (q_h, q_k, q_l) (in units of Å^{-1}) as $(h, k, l) = (q_h a/2\pi, q_k b/2\pi, q_l c/2\pi)$ in reciprocal lattice units (r.l.u.), where $a = 3.82$, $b = 3.88$ and $c = 11.68$ Å are lattice parameters [10]. (a) Schematic diagram for YBCO. (b) The l-dependence of acoustic and optical spin fluctuations for $E_i = 200$ meV. (c) Dispersion of constant energy peaks in $\chi_o''(\mathbf{Q}, \omega)$. The orientation of incommensurate peaks is shown in the inset. (d) Dispersion constant energy peaks in $\chi_a''(\mathbf{Q}, \omega)$. The solid line shows spin-wave dispersion from undoped YBa$_2$Cu$_3$O$_{6.15}$ (Ref. [20, 21]). The inset shows the orientation of the incommensurate spin fluctuations below the resonance energy. (e),(f) Local susceptibility of 100 K-15 K for optical $\chi_a''(\omega)$ and acoustic $\chi_o''(\omega)$ modes in absolute units. The red circles and black squares are obtained with cuts along the $(h, 1 - h)$ and (h, h) directions with an integrating width of ± 0.15 rlu, respectively. The inset in (e) shows hole-doping dependence of the optical "resonance" with the red circle and the green triangle from Refs. [23, 24]. The vertical error bars in (c),(d) and the horizontal error bars in (e),(f) indicate the energy integration range. The vertical error bars in (e) and (f) are statistical uncertainties (1σ).

dence of the $34 \leq \hbar\omega \leq 44$ meV scattering at the position of optical spin fluctuations ($E_i = 90$ meV). A clear incommensurate scattering appears at 15 K (Fig. 2(a)) and they are replaced by a broad response at 100 K (Fig. 2(b)). Figs. 2(d)-(f) show the temperature dependence of the scattering around the 41 meV acoustic resonance obtained by using $E_i = 210$ meV. At $T = 15$ K, the scattering shows a sharp resonance centered at $(1/2, 1/2)$ [10]. On warming to 100 K, the resonance disappears
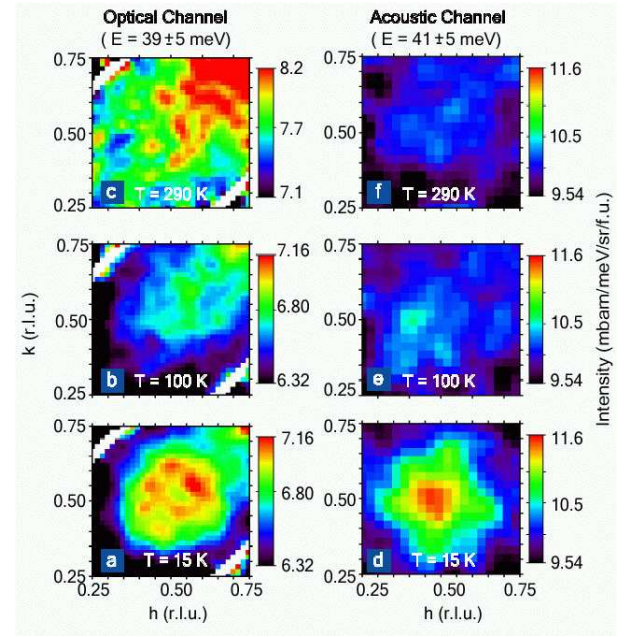

FIG. 2: The temperature dependence of the magnetic scattering around $\hbar\omega \approx 40$ meV at optical (d)-(f), $Ei = 90$ meV, and acoustic (a)-(c), $E_i = 210$ meV. A clear commensurate magnetic scattering is seen at $\sim$40 meV at 15 K in (d) while (a) shows incommensurate scattering. The intensity of phonons increases with increasing temperature and wavevector (e),(f).

(Fig. 2(e)). Further warming to 290 K does not change the scattering significantly (Fig. 2(f)).

Figure 3 summarizes the optical spin fluctuations for $31 \leq \hbar\omega \leq 75$ meV. For $31 \leq \hbar\omega \leq 34$ meV, the scattering shows no difference between normal and superconducting states (Figs. 3(a) and 3(e)). Since there is little normal state magnetic scattering, there must be an optical spin gap around 34 meV. On increasing the energy transfer to $\hbar\omega = 39 \pm 5$ meV, where the acoustic channel has a commensurate resonance, spin fluctuations in the optical channel form a broad incommensurate structure away from $(1/2, 1/2)$ (Fig. 3(b)). Figure 4f confirms the incommensurate nature of the scattering and shows that the (h, h) and $(h, 0.5)$ cut directions are inequivalent. For $\hbar\omega = 52 \pm 5$ meV, again we find incommensurate peaks but this time the scattering is more box-like with enhanced corners (Figs. 3(c) and 3(g)). The orientation of the scattering is rotated 45° from that in Fig. 4(b), similar to acoustic high-energy spin excitations in YBa$_2$Cu$_3$O$_{6.6}$ [12]. Finally, on moving the energy to $\hbar\omega = 66 \pm 9$ meV, the temperature difference spectrum is featureless. Inspection of the unsubtracted data at 15 K reveals no observable magnetic scattering (Fig. 3(h)).

Figures 4(a)-(e) show the intensity difference spectra between 15 K and 100 K at various energies in the acoustic channel. For $20 \leq \hbar\omega \leq 27$ meV, the temperature difference has negative intensity, possibly due to a reduction in the magnetic response on entering the superconduct-
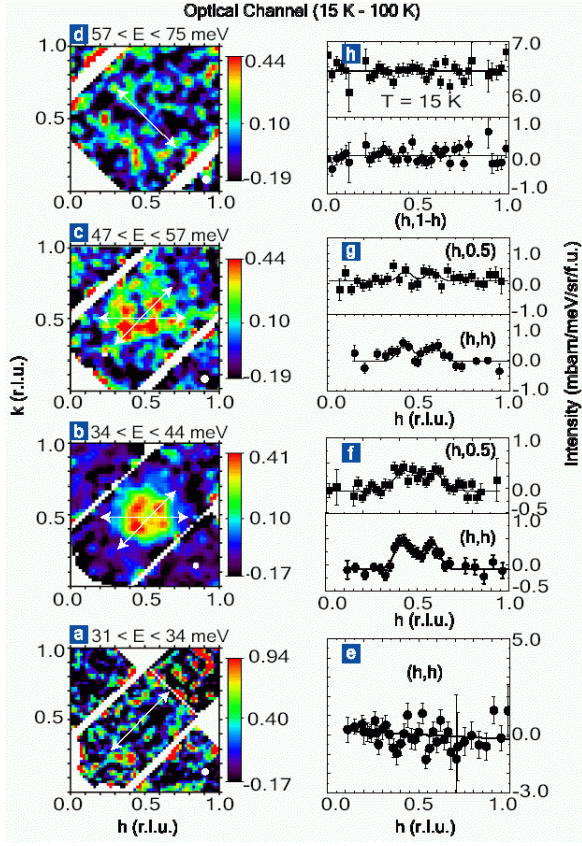
FIG. 3: Temperature difference (15 K−100 K) at various energies for optical mode defined as scattering with $\cos^2(q_z d/2) > 0.8$. Images (a)-(d) are obtained with $Ei = 75, 90, 130, 210$ meV, respectively. The image at $\hbar\omega = 45.5 \pm 1.5$ meV does not have enough statistics to determine the **Q**-structure. Panels (e)-(h) are cuts with $\hbar\omega = 32.5 \pm 1.5, 39 \pm 5, 52 \pm 5, 66 \pm 9$ meV, respectively. The upper panel of (h) shows a cut through the unsubtracted data of (h) at 15 K. The vertical error bars in (e-h) are statistical uncertainties (1σ).

FIG. 4: Temperature difference spectra (15 K−100 K) at various energies for acoustic mode defined as any scattering with $\sin^2(q_z d/2) > 0.8$ (see Fig. 1d). Images (a)-(e) are obtained with $Ei = 90, 210, 210, 90, 110$ meV, respectively. Cuts in (f)-(j) are obtained with $\hbar\omega = 41 \pm 5, 31 \pm 4, 40 \pm 5, 55.5 \pm 3.5, 64.5 \pm 4.5$ meV, respectively. The upper panel of (j) shows a cut through the unsubtracted data of (e) at 15 K. The instrumental Q-resolutions are marked by white circles in (a)-(e). The vertical error bars in (f-j) are statistical uncertainties (1σ).

ing state [19] or large phonon population at 100 K (Fig. 4a). A cut through the image confirms no intensity gain at low temperatures (Fig. 4f). When increasing the energy to $27 \leq \hbar\omega \leq 35$ meV, the difference image shows a quartet of incommensurate peaks at $(1/2 \pm \delta, 1/2)$ and $(1/2, 1/2 \pm \delta)$ with $\delta = 0.11 \pm 0.02$ r.l.u. To demonstrate that the incommensurate scattering is not circular around $(1/2, 1/2)$, we made two cuts through the image. The cut along the $(h, 1/2)$ direction clearly shows two incommensurate peaks around $(1/2, 1/2)$. In contrast, a cut along the $(h, 1-h)$ direction has no incommensurate peaks. Note that a circular symmetry at $\hbar\omega = 35$ meV has been suggested for YBCO from previous triple-axis experiments [18].

Figure 4(c) shows the data at the resonance energy and its wavevector dependence has a Gaussian lineshape centered around $(1/2, 1/2)$ (Fig. 4(h)). For energies above the resonance ($52 \leq \hbar\omega \leq 59$ meV), the scattering is in-
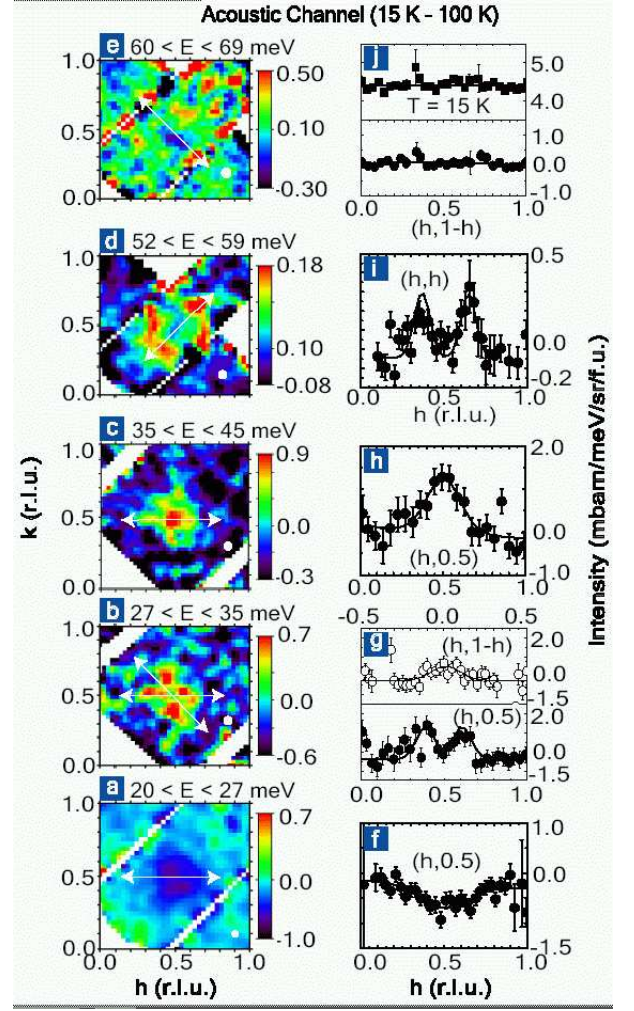
commensurate although the low counting rate does not allow an unambiguous identification of its **Q**-structure (Figs. 4(d),4(i)). For $\hbar\omega > 60$ meV, the temperature difference spectra as well as unsubtracted data show no evidence of magnetic scattering around $(1/2, 1/2)$ (Figs. 4(e),4(j)).

Figures 1(e) and 1(f) summarize the superconductivity-induced (15 K−100 K) change in the local dynamic susceptibility $\chi''(\omega)$ in absolute units for optical and acoustic channels of YBCO, respectively. In the optical channel, $\chi''_o(\omega)$ has a peak at $\hbar\omega = 46$ meV, similar to theoretical expectations [25]. The

magnetic spectral weight gradually increases from above the spin-gap value of $\sim$30 meV [10], peaks at 46 meV, and finally diminishes for energies above $\sim$70 meV. The acoustic channel behaves similarly although it peaks at the expected resonance position of 40 meV [10]. The magnitude of the total spectral weight in the optical channel $\left\langle m^2 \right\rangle_{op} = 0.078 \pm 0.02 \; \mu_B^2$ and in the acoustic channel is $\left\langle m^2 \right\rangle_{ac} = 0.102 \pm 0.02 \; \mu_B^2$ per f.u. respectively. This value is similar to that for $YBa_2Cu_3O_{6.6}$ around the acoustic resonance energy ($\left\langle m^2 \right\rangle_{ac} = 0.12 \pm 0.02 \; \mu_B^2$/f.u. for $24 < \hbar\omega < 44$ meV) [12]. Since the high-energy response in underdoped $YBa_2Cu_3O_{6+x}$ ($x = 0.5, 0.6$) takes up much more spectral weight than the resonance [11, 12], it is surprising that there is essentially no observed magnetic response for energies above 60 meV in YBCO (Fig. 1f). Compared to undoped $YBa_2Cu_3O_{6.15}$ [20, 21], which has a total integrated moment of $\sim$0.4 μ_B^2/f.u. when integrated up to 120 meV, the total integrated moment in optimally doped YBCO has only about 26% of the spectral weight in the same energy range in the acoustic channel only.

Using the spin excitation spectra in Figs. 3 and 4, we have calculated the changes in the magnetic excitations from the normal to the superconducting state and estimated $\delta \left\langle \vec{S}_i \cdot \vec{S}_j \right\rangle = -0.020 \pm 0.008$/f.u., where $\left\langle \vec{S}_i \cdot \vec{S}_j \right\rangle$ is the spin-spin correlation function for nearest neighbour copper atoms (see supplementary information). This estimate neglects contributions from energies below 24 meV and above 70 meV, where magnetic scattering is difficult to resolve. Also, in Eq. (1) the difference between normal and superconducting state is meant to be determined at the same temperature, while here we had to take normal state data at 100 K and superconducting state data at 15 K neglecting a possible temperature dependence of the normal state magnetic excitations. In order to assess the error introduced by these neglections, we have fitted an RPA-BCS model calculation of the spin excitation spectrum [22] to our data and calculated the missing contributions within this model. This calculation indicates that our value for ΔE_{ex} could be of order 30 % too large due to these neglections(see supplementary information).

Assuming an exchange coupling of $J = 100$ meV, the change in exchange energy would be $\Delta E_{ex} = 2J \, \delta \left\langle \vec{S}_i \cdot \vec{S}_j \right\rangle = -4.1$ meV/f.u.=-24 K/planar Cu. This value is a factor of 1.3 times larger than the 18 K/Cu estimated from the acoustic resonance alone in previous work [4]. Even if we consider that our estimation may be too large by 30 %, the change in the exchange energy is still much larger than the $U_0 \cong 25(J/mole) \simeq 0.26$ meV/f.u.= 3 K/f.u. = 1.5 K/planar Cu condensation energy [15, 16].

Our results reveal two important conclusions for spin excitations of optimally doped YBCO. First, the optical resonance reported earlier [23, 24] is actually incommensurate and this naturally explains the large Q-widths previously reported. Second, our determination of the dynamical susceptibility in absolute units allows an estimation of the change of the magnetic excitation energy available to the superconducting condensation energy [4, 14, 26]. We find that the magnetic exchange energy is about 15 times larger than that of the superconducting condensation energy, thus indicating magnetism can be the driving force for electron pairing and superconductivity.

[1] Scalapino, D. J. The case for $d_{x^2-y^2}$ pairing in the cuprate superconductors. Phys. Reports **250**, 330-365 (1995).

[2] Chubukov, A., Pines, D., & Schmalian, J., in The Physics of Superconductors, Vol I, Conventional and High-T_c Superconductors (ed. by Bennemann, K.H. & Ketterson, J.B.) 495-590 (Springer, Berlin, 2003).

[3] Scalapino, D. J. & White, S. R. Superconducting condensation energy and an antiferromagnetic exchange-based pairing mechanism. Phys. Rev. B **58**, 8222-8224 (1998).

[4] Demler, E. & Zhang, S-C. Quantitative test of a microscopic mechanism of high-temperature superconductivity. Nature **396**, 733-735 (1998).

[5] Maier, Th. A. On the nature of pairing in the two-dimensional t-J model. Physica B **359-361**, 512-514 (2005).

[6] Rossat-Mignod, J. *et al.* Neutron scattering study of the $YBa_2Cu_3O_{6+x}$ system. Physica C **185**, 86-92 (1991).

[7] Mook, H. A. *et al.* Polarized neutron determination of the magnetic excitations in $YBa_2Cu_3O_7$. Phys. Rev. Lett. **70**, 3490-3493 (1993).

[8] Mook, H. A. *et al.* Spin fluctuations in $YBa_2Cu_3O_{6.6}$. Nature **395**, 580-582 (1998).

[9] Fong, H. F. *et al.* Spin susceptibility in underdoped $YBa_2Cu_3O_{6+x}$. Phys. Rev. B **61**, 14773-14786 (2000).

[10] Dai, P., Mook, H. A., Hunt, R. D., & Doğan, F. Evolution of the resonance and incommensurate spin fluctuations in superconducting $YBa_2Cu_3O_{6+x}$. Phys. Rev. B **63**, 054525 (2001).

[11] Stock, C. *et al.* From incommensurate to dispersive spin-fluctuations: The high-energy inelastic spectrum in superconducting $YBa_2Cu_3O_{6.5}$. Phys. Rev. B **71**, 024522 (2005).

[12] Hayden, S. M., Mook, H. A., Dai, P., Perring, T. G., & Doğan, F. The structure of the high-energy spin excitations in a high-transition-temperature superconductor. Nature **429**, 531-534 (2004).

[13] Dai, P. *et al.*, The magnetic excitation spectrum and thermodynamics of high-T_c superconductors. Science **284**, 1344-1347 (1999).

[14] Kee, H-Y., Kivelson, S. A. & Aeppli, G. Spin-1 Neutron Resonance Peak Cannot Account for Electronic Anomalies in the Cuprate Superconductors. Phys. Rev. Lett. **88**, 257002 (2002).

[15] Loram, J. W., Mirza, K. A., Cooper, J. R. & Tallon, J. L. Specific heat evidence on the normal state pseudogap, J. Phys. Chem. Solids. **59**, 2091-2094 (1998).

[16] Lortz, R. *et al.* Evolution of the specific-heat anomaly

of the high-temperature superconductor in $YBa_2Cu_3O_7$ under the influence of doping through application of pressure up to 10 GPa. J.Phys.: Condens. Matter **17**, 4135-4145 (2005).

[17] Woo, H. *et al.* Mapping spin-wave dispersions in stripe-ordered $La_{2x}Sr_xNiO_4$ ($x = 0.275, 0.333$). Phys. Rev. B **72**, 064437 (2005).

[18] Reznik, D. *et al.* Dispersion of Magnetic Excitations in Optimally Doped Superconducting $YBa_2Cu_3O_{6.95}$. Phys. Rev. Lett. **93**, 207003 (2004).

[19] Regnault, L. P. *et al.* Spin dynamics in the high-T_c superconducting system $YBa_2Cu_3O_{6+x}$. Physica B **213 & 214**, 48-53 (1995).

[20] Hayden, S. M. *et al.* High-frequency spin waves in $YBa_2Cu_3O_{6.15}$. Phys. Rev. B **54**, R6905-R6908 (1996).

[21] Reznik, D. *et al.* Direct observation of optical magnons in $YBa_2Cu_3O_{6.2}$. Phys. Rev. B **53**, R14741-R14744 (1996).

[22] Dahm, T. *et al.*, Nodal quasiparticle lifetimes in cuprate superconductors. Phys. Rev. B **72**, 214512 (2005).

[23] Pailhes, S. *et al.* Resonant Magnetic Excitations at High Energy in Superconducting $YBa_2Cu_3O_{6.85}$. Phys. Rev. Lett. **93**, 167001 (2004).

[24] Pailhes, S. *et al.* Two Resonant Magnetic Modes in an Overdoped High T_c Superconductor. Phys. Rev. Lett. **91**, 237002 (2003).

[25] Chen, W. Q. & Weng, Z. Y. Spin dynamics in a doped-Mott-insulator superconductor. Phys. Rev. B **71**, 134516 (2005).

[26] Chakravarty, S. & Kee, H-Y. Measuring condensate fraction in superconductors. Phys. Rev. B **61**, 14821-14824 (2000).

Competing financial interests

The authors declare that they have no competing financial interests.